

9/

UNIDIRECTIONAL SOLIDIFICATION OF
Al-CuAl₂ EUTECTIC

Kwame Ankra
(M. S. Thesis)

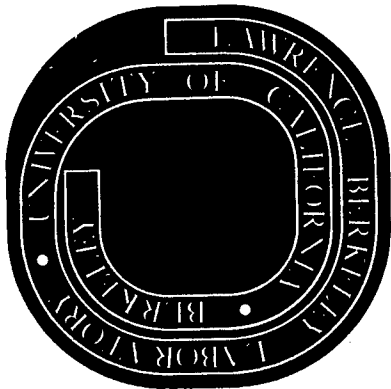
December 1972

RECEIVED
LAWRENCE
BERNARD LABORATORY

GENERAL AND
ADMINISTRATIVE SECTION

Prepared for the U. S. Atomic Energy
Commission under Contract W-7405-ENG-48

For Reference
Not to be taken from this room



DISCLAIMER

This document was prepared as an account of work sponsored by the United States Government. While this document is believed to contain correct information, neither the United States Government nor any agency thereof, nor the Regents of the University of California, nor any of their employees, makes any warranty, express or implied, or assumes any legal responsibility for the accuracy, completeness, or usefulness of any information, apparatus, product, or process disclosed, or represents that its use would not infringe privately owned rights. Reference herein to any specific commercial product, process, or service by its trade name, trademark, manufacturer, or otherwise, does not necessarily constitute or imply its endorsement, recommendation, or favoring by the United States Government or any agency thereof, or the Regents of the University of California. The views and opinions of authors expressed herein do not necessarily state or reflect those of the United States Government or any agency thereof or the Regents of the University of California.

0.04
0.02

Table of Contents

ABSTRACT v

I. INTRODUCTION 1

II. ORIGINS OF BANDING FROM NATURAL CONVECTION 4

III. EXPERIMENTAL 8

IV. RESULTS 14

V. ANALYSIS AND DISCUSSION 30

 A. Band Density Distributions 30

 B. Transient Interface Condition During Banding 33

 C. Subgrain Density Dependence on Band Spacing 39

 D. Effect of Flow Separation of Variable Band Width 40

 E. Dendritic Breakdown of the Eutectic 41

VI. CONCLUSION 42

ACKNOWLEDGEMENTS 43

REFERENCES 44

UNIDIRECTIONAL SOLIDIFICATION OF Al-CuAl₂ EUTECTIC

Kwame Ankra

Inorganic Materials Research Division, Lawrence Berkeley Laboratory and
Department of Materials Science and Engineering, College of Engineering;
University of California, Berkeley, California

ABSTRACT

Banded microstructures have been studied in the Al-CuAl₂ eutectic unidirectionally solidified at large velocities (ca. 200 cm/hr) in a horizontal open mold. Some new types of banding have been observed including a lamellar-to-dendrite breakdown. Some of these phenomena could not be explained by current theories. The microstructures are analyzed and related to a proposed mechanism for their occurrence based on convection currents in the melt.

I. INTRODUCTION

The presence of regular inhomogeneities of a planar nature in crystals, such as in the index of refraction, resistivity, and other properties is usually called "banding" which may be visible on low magnification photomicrographs of the polished and etched surfaces. In the absence of impurities or dopants, the bands represent changes in stoichiometry which can be caused by irregular convection^{1,2} during solidification in which case the bands are parallel to the growing melt-solid interface (perpendicular to the growth direction). In other words, a transverse banded structure results. When constitutional supercooling is a problem, facets, cellular interfaces and, in the limit, dendritic structures result. In this case the bands are parallel to the growth direction.

It has been shown that thermal convection always exists in any fluid where the temperature gradient is not aligned in the direction of gravity. The existence of such convection currents in the melt has been known to affect the solidification process in the following ways:⁵

i. Movement of the melt can modify the rate of heat transfer at the melt-solid interface and hence the actual solidification rate.

ii. It can influence the structure of the solid formed, in particular, the transition from columnar to equiaxed structure, and finally

iii. It would also affect the solute distribution in multi-component systems. Thus natural convection affects both the structure of the solid formed and the rate at which solidification occurs.

Banding which results from irregular convection can be partially suppressed through the application of magnetic fields.^{3a,3b}

Earlier investigations of the Al-CuAl₂ eutectic seemed to have shown that banding is only observed at rates of growth less than 20 cm/hr.^{6,7} This upper limit on non-banded solidification is inferred from the fact that the maximum solidification velocity used by Kraft et al.⁶ was 16.70 cm/hr. Kraft explained the upper limit based upon the hypothesis that "extremely slow solidification rates" allowed impurity build-ups that upon precipitating causes one or both phases to freeze laterally. Faster solidification rates on the other hand, do not give sufficient time for such impurity build-ups and hence the banding phenomenon is not observed.

As it was stated above, convection currents within the melt can affect the actual rate at which solidification occurs. It should therefore be possible to observe banding at higher growth velocities in the presence of convection currents within the melt. Chadwick⁷ has shown that banding can be mechanically induced by changes in the actual solidification rate. In his investigation of the banding phenomenon subsequent to the experiments of Kraft et al.⁶ at slow growth rates, Chadwick⁷ found that the structure could be induced at will by slightly increasing or decreasing the growth rate momentarily from the steady state rate of growth. He then concluded that banding effect was due to minor perturbations on otherwise steady state conditions of growth. It should not matter whether the changes in solidification rates was convection current induced or mechanically induced.

The present study was undertaken to explore the banding process in lamellar eutectics at high solidification velocity. It will be shown that banding is possible even at high growth velocities > 20 cm/hr since the rate of solidification is not the only determining factor, the band spacing will be correlated with possible thermal instabilities by measuring the λ spacing variation in the region of a band. Some microstructures will be reported which to the writer's knowledge, have not been hitherto observed. Their occurrence is attributed to the convectional currents within the melt based on a model proposed. The contribution of convectional currents to the banding process is included by carrying out directional solidification experiments in a direction perpendicular to that of gravity.

II. ORIGINS OF BANDING FROM NATURAL CONVECTION

There have been many studies done on natural convection in purely liquid systems.⁹⁻²² However, fluid flow during horizontal crystal growth has only recently been the subject of experimental investigation.²³⁻³³ From these studies, the flow pattern has been established^{3,23,33} to be circulatory, directed toward the interface at the surface of the liquid, down and away from the interface at the bottom, and then up at the hot end of the melt. During crystal growth, such a flow may interact with a solute boundary layer at the solid-liquid interface to affect solute incorporation.^{23-28,34,35} With the increase in temperature gradient, or solid-liquid interface height, laminar fluid flow ensues and heat transport takes place by laminar convection, as well as by conduction. Turbulent heat transfer takes place at higher values of these temperature gradients and interface variables. In the transition region between laminar and turbulent flow, boundary layer separation can take place; fluctuations in temperature are then observable and these increase in amplitude and frequency as turbulence becomes dominant. These temperature oscillations are known to be a direct result of the flow instabilities of which these are two types:

- (1) Carruthers and Winegard²⁴ observed the occurrence of boundary layer separation at corners in horizontal melting configurations, and
- (2) Bénard instabilities have been observed under inverted vertical temperature gradients.

The temperature oscillations have been investigated both theoretically and experimentally by earlier workers.^{23,26,28,32}

In a recent study by Vandenbulcke and Vuillard,² two intermediate types of convection were found during vertically downward eutectic solidification in the transition region. These were the "laminar-laminar" convection where the perturbations quickly pass from the laminar region to a much faster laminar region and progressively returning to a much slower laminar region. These authors also reported a "laminar-turbulent" region where convection alternates between periods of laminar convection and turbulent convection. These convectional currents were accompanied by the temperature oscillations characteristic of each region. With the exception of the pure laminar region, all the others resulted in banded microstructures.

Thermal convection in rectangular enclosures was first treated by Batchelor²¹ for two dimensional configuration shown in Fig. 14 (after Carruthers).⁴ By assuming steady state, Batchelor combines two equations of fluid motion to get:

$$\begin{aligned} & \frac{1}{N_{pr}} \left[\frac{\partial w}{\partial x} \frac{\partial \psi}{\partial y} - \frac{\partial w}{\partial y} \frac{\partial \psi}{\partial x} \right] \\ &= \frac{1}{N_{pr}} \frac{\partial(w, \psi)}{\partial(x, y)} \\ &= N_{Ra} \frac{\partial \theta}{\partial y} + \nabla_w^2 \end{aligned}$$

where the velocities in the x and y directions have been defined as

$U = (k/d) \partial\psi/\partial y$ and $V = -(K/d) \partial\psi/\partial x$ respectively, ψ being a

dimensionless stream function. The length variables x, y are dimensionless in units of d . The symbols used are:

- k = thermal diffusivity
- Θ = Dimensionless temperature = $\frac{T - T_o}{T_1 - T_o}$
- N_{pr} = Prandtl number = ν/k
- N_{Ra} = Rayleigh number = $g\beta(T_1 - T_o)d^3/\nu^2$
- β = Liquid coefficient of thermal expansion.
- g = gravitational constant.
- ν = Kinematic viscosity.
- w = dimensionless vorticity = $\nabla^2\psi$
- T_1, T_o = Hot and cold wall temperatures respectively.

The steady state equation is

$$\frac{\partial(\theta, \psi)}{\partial(x, y)} = \nabla^2\theta$$

The boundary conditions for the vertical boundaries are:

$$\begin{aligned} \psi = \partial\psi/\partial y = 0, & \quad \theta = 0 \text{ at } y = 0 \\ \psi = \partial\psi/\partial y = 0, & \quad \theta = 1 \text{ at } y = 1.0 \end{aligned}$$

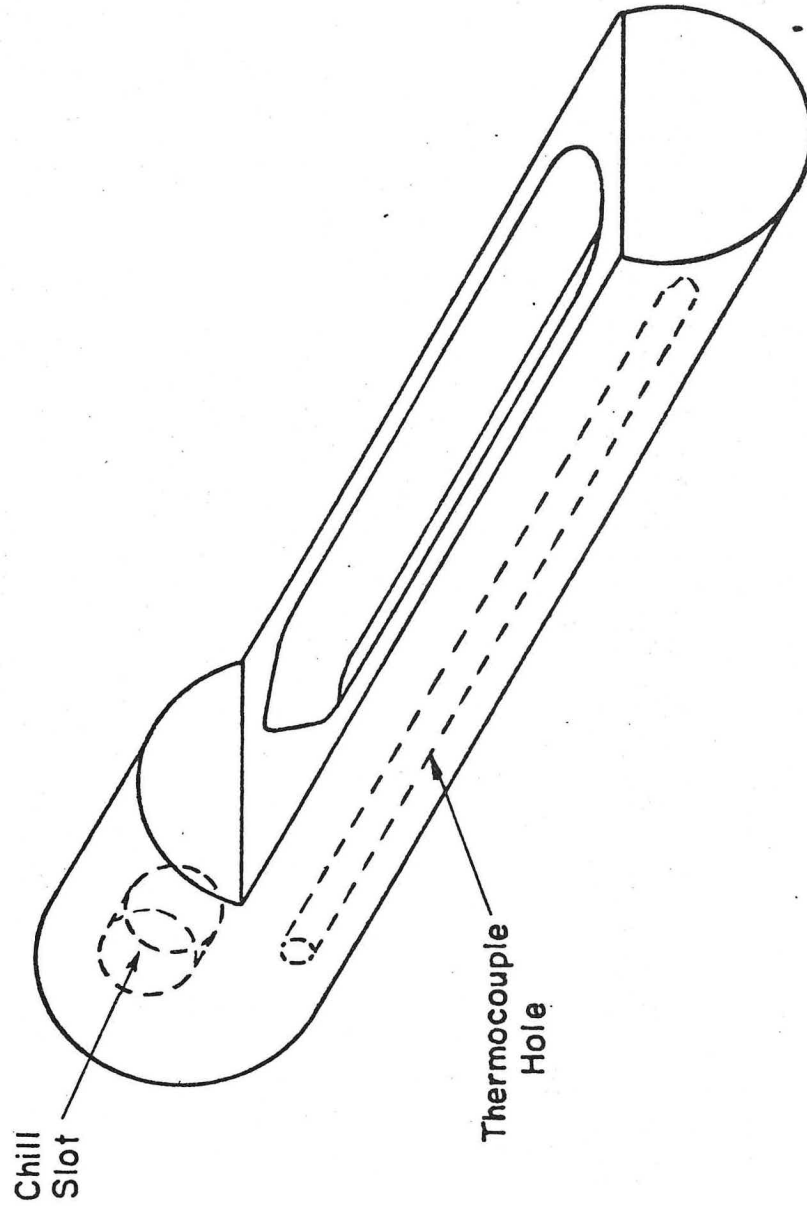
The horizontal boundary conditions used by most workers range from the extremes

$$\begin{aligned} \psi = \partial\psi/\partial x = 0 \text{ and } \theta = y & \quad \text{at } x = 0; 1/\ell \\ \psi = \partial\psi/\partial x = 0 \text{ and } \frac{\partial\theta}{\partial y} = 0 & \quad \text{at } x = 0; 1/\ell \end{aligned}$$

If thermal instabilities resulting from the convection currents within the melt produce bands then the length of the liquid zone is important. Long liquid zones should support turbulent convection and produce closely spaced bands whilst short zones should produce fewer, widely spaced bands. Eventually as the zone length becomes very short the bands produced by thermal instabilities should disappear.

III. EXPERIMENTAL

Ten high purity (99.999%) Al-Cu eutectic alloys were prepared by melting the component metals together in a carbon crucible under argon. The alloys, after complete homogenization, were solidified unidirectionally in an open, rectangular graphite mold under an argon atmosphere. A very steep temperature gradient estimated to be $206 \pm 8^\circ\text{C}/\text{cm}$ was maintained with a furnace travel rate of 216 cm/hr and a maximum temperature of 1000°C . The solidification apparatus comprised a horizontal resistance furnace mounted on rollers and attached to a variable speed motor capable of providing very wide variations of linear travel of the furnace with respect to the fixed mold. A chromel-alumel thermocouple placed within the mold and attached to a chart recorder monitored the temperature profile of the mold during growth. The mold was constructed with a water-cooled copper coil inserted into one end at which solidification was to begin. The apparatus is shown in Fig. 1. This construction serves to give a planar solid-liquid interface and to produce a stable high temperature gradient in the liquid ahead of the interface.⁷ The end of the mold where solidification was to begin was V-shaped to aid nucleation. This arrangement explains why one could obtain the stable lamellar morphology under the high growth rates studied. Furnace travel rates were varied from 10.8 to 216 cm/hr. It was assumed that the moving furnace produced a constant temperature gradient ahead of the solid-liquid interface over most of the length of the specimen and that the rate of furnace travel was equal to the rate of advance of the solid-liquid interface. After directional



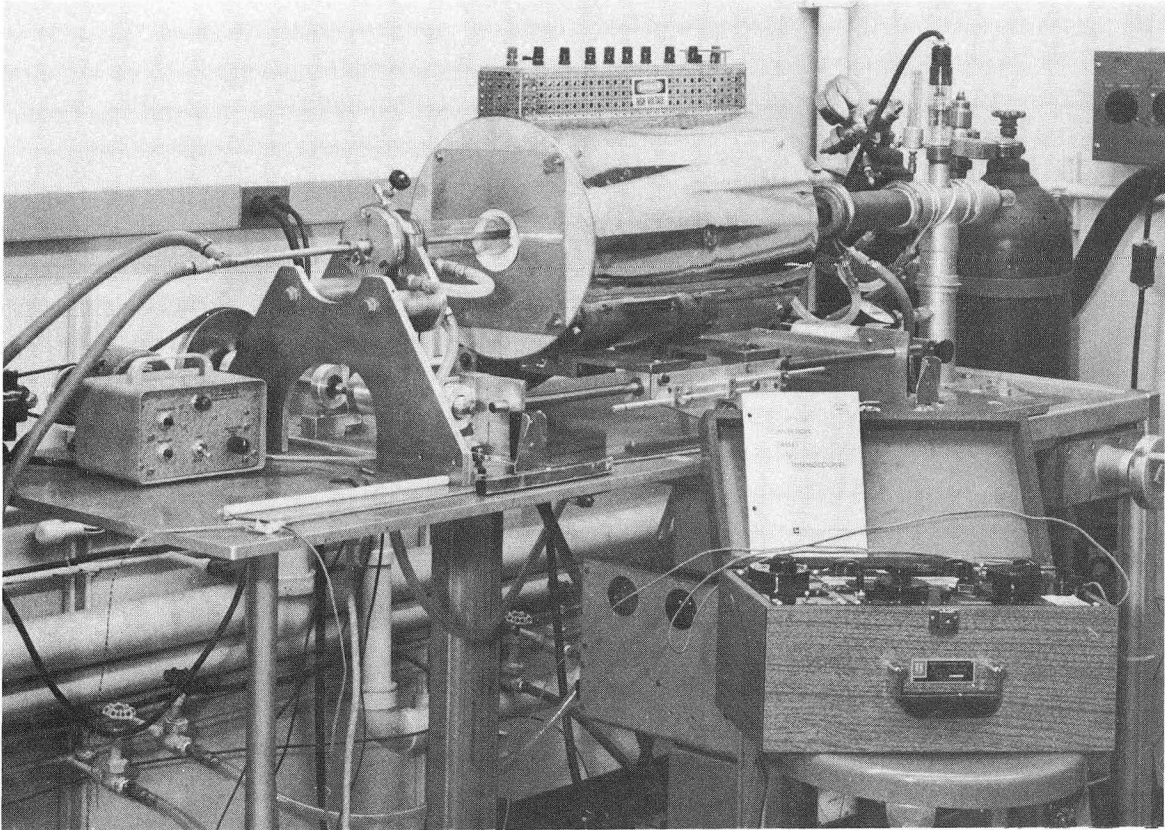
XBL 7212-7369

Fig. 1(a). Eutectic Solidification Boat.



XBB 722-1216

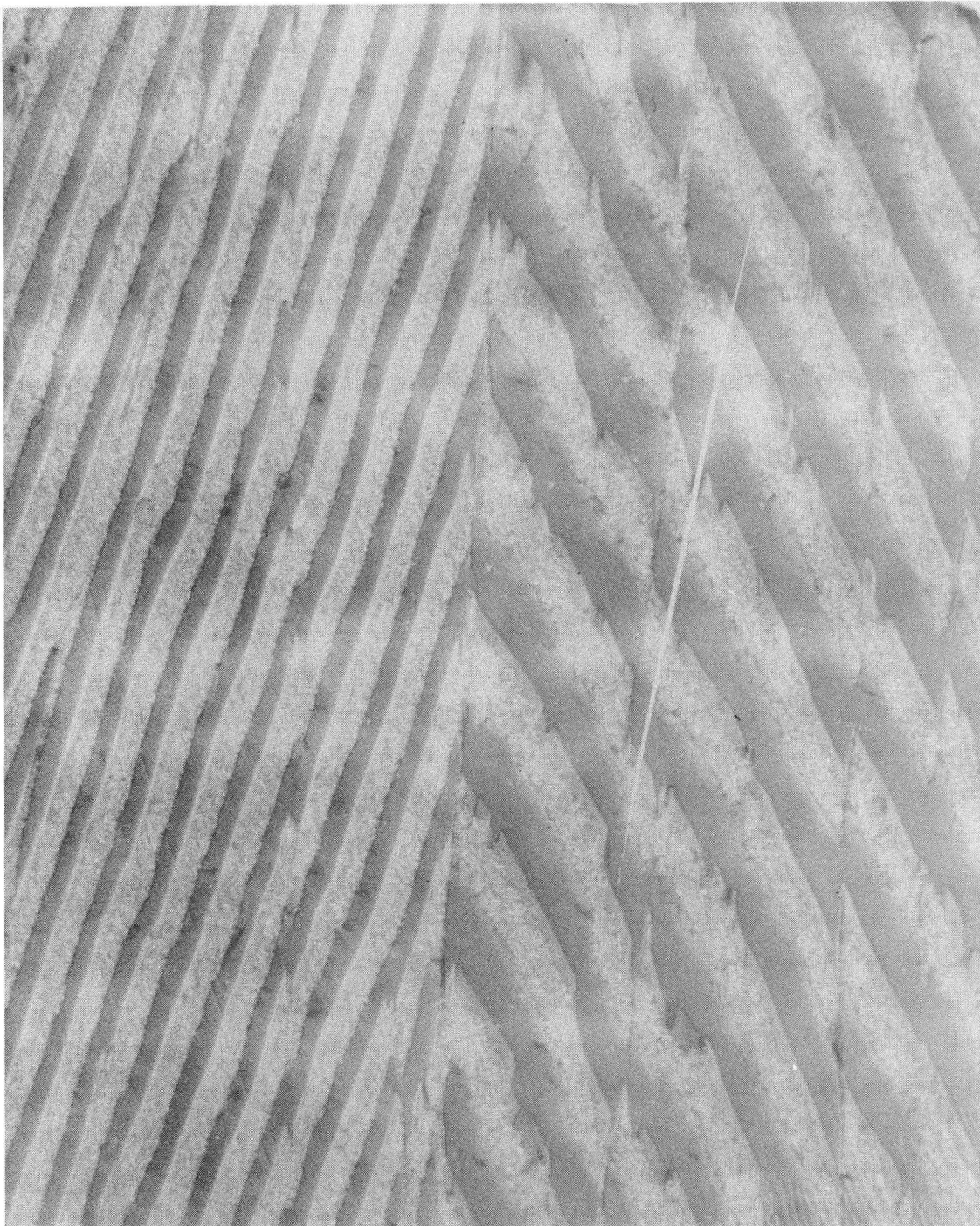
Fig. 1(b). Apparatus for solidification.



XBB 722-1216

Fig. 1(c). Apparatus for solification: expanded view of horizontal furnace.

solidification each of the ten samples was sectioned horizontally to reveal the microstructure parallel to the direction of freezing, and sectioned perpendicular to the freezing direction to reveal the transverse microstructure. All microstructures shown in Figs. 2-13 were directionally solidified at 216 cm/hr. The growth velocity of Fig. 14 was 10.8 cm/hr. Unless otherwise indicated, the transverse microstructures came from approximately 6 cm from the specimen end where solidification began. There was no erratic motion of the furnace and other experiments had eliminated other possible mechanical and electrical sources. If it is supposed that there was such erratic motion of the furnace, it is quite clear that at the high growth rate used, the effect of such motion would be practically unobservable. There was no cooling rate variation since the water flow was regulated by a flow meter.



XBB 7210-5213

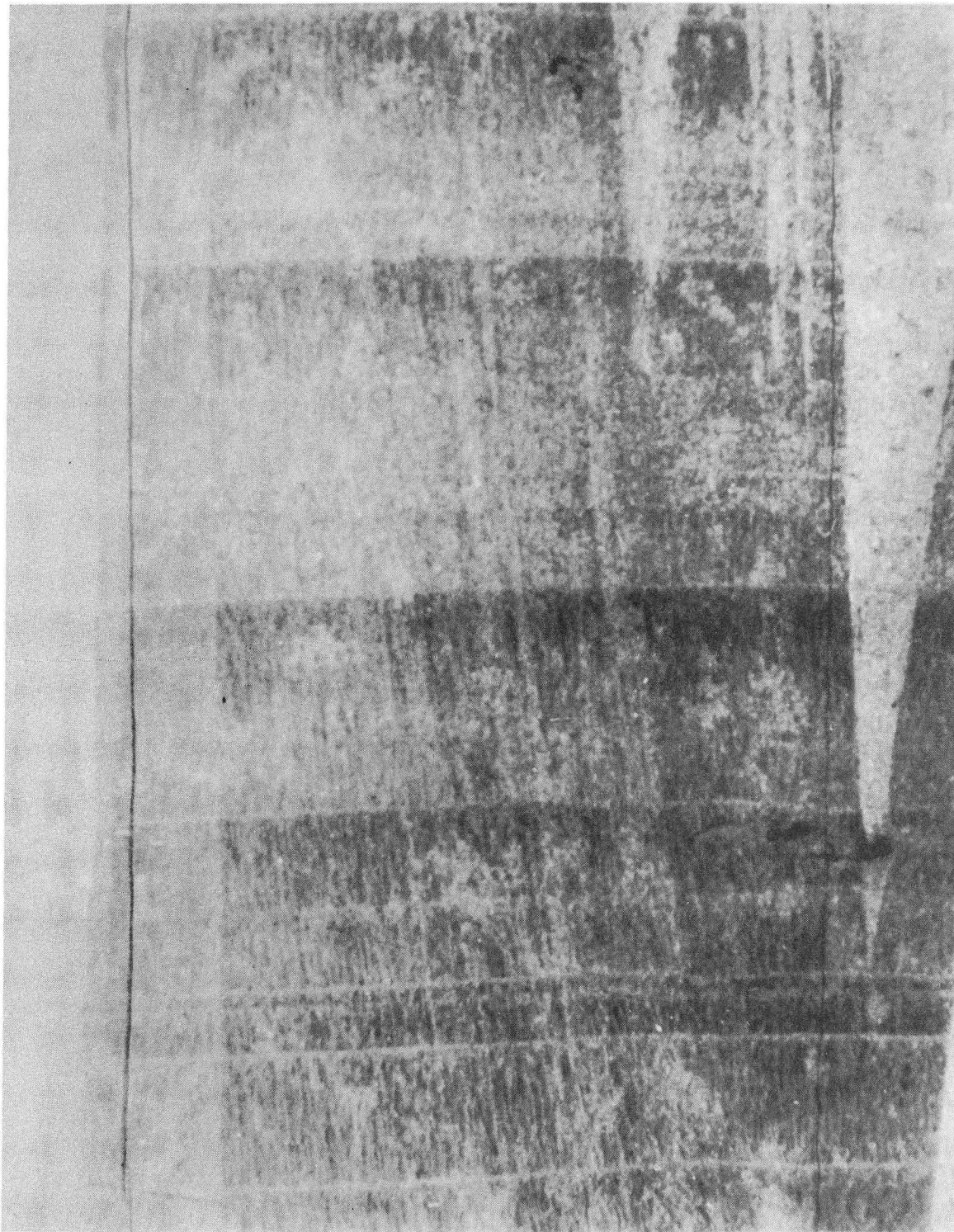
Fig. 14. Longitudinal section of unidirectionally solidified Al-CuAl₂ eutectic showing two grains.
Mag. 1360x Growth rate equals 10.8 cm/hr.

IV. RESULTS

Each of the ten directionally solidified specimens showed the transverse banding phenomenon to the unaided eye when polished and etched in longitudinal section. Each showed evidence of multiple grains extending along the length of the specimen in the direction of freezing, the grain size generally increasing with distance from the seed end. The transverse sections showed the equilibrium, regularly spaced lamellar structure of the Al-CuAl₂ eutectic, while others exhibited a highly disordered subgrain structure.

The banding structure differed both in density and band width, with the band density tending to decrease with distance along each of the specimens in the direction of solidification. The band structure observed in the specimens could be separated into three distinct types. In several specimens the bands were narrow with the regular lamellar structure predominating in the regions between the bands. In other specimens the bands varied in width along the band and a high subgrain density persisted along their length. In three of the specimens a clear dendritic breakdown of the eutectic lamellar structure was observed. The dendritic structure was followed by a branched cellular structure.

The transverse section of a typical specimen showing wide bands is shown in Fig. 2. Since the band records a solidification velocity transient on the solid-liquid interface, and since this interface is essentially isothermal, the temperature profile along the specimen can be inferred from the curvature of the bands. The isotherms are convex toward the liquid, and the curvature is clearly greater toward the edge



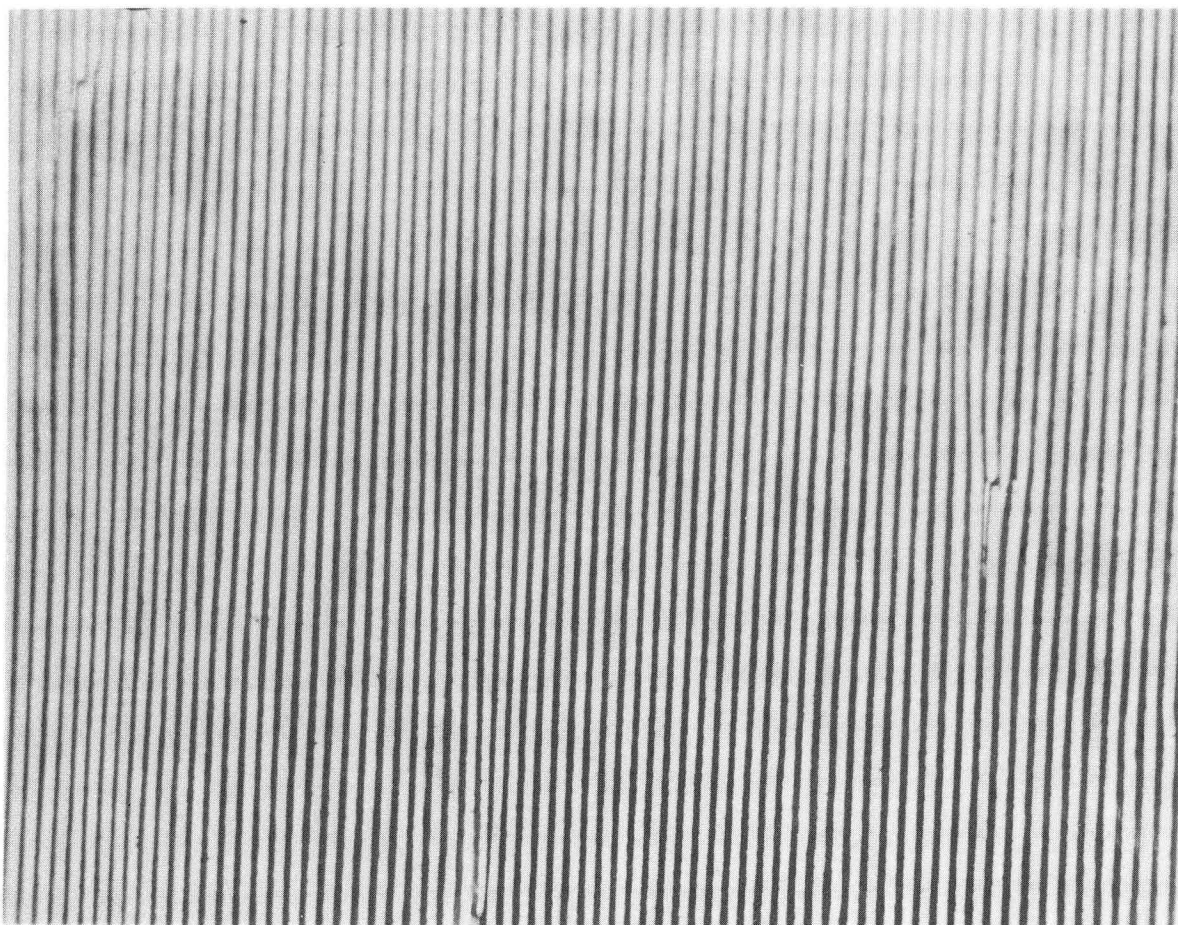
XBB 7210-5211

Fig. 2. Typical banded structure visible to the unaided eye. Mag. 45x
Growth direction is from bottom to top.

of the mold. In contrast, the thermal profile observed by Kraft et al⁶ was concave toward the melt from which Kraft concluded that the curvature was produced by efficient heat extraction by the water chill. In the micrograph shown in Fig. 2 the isotherms are essentially linear through some of the grains.

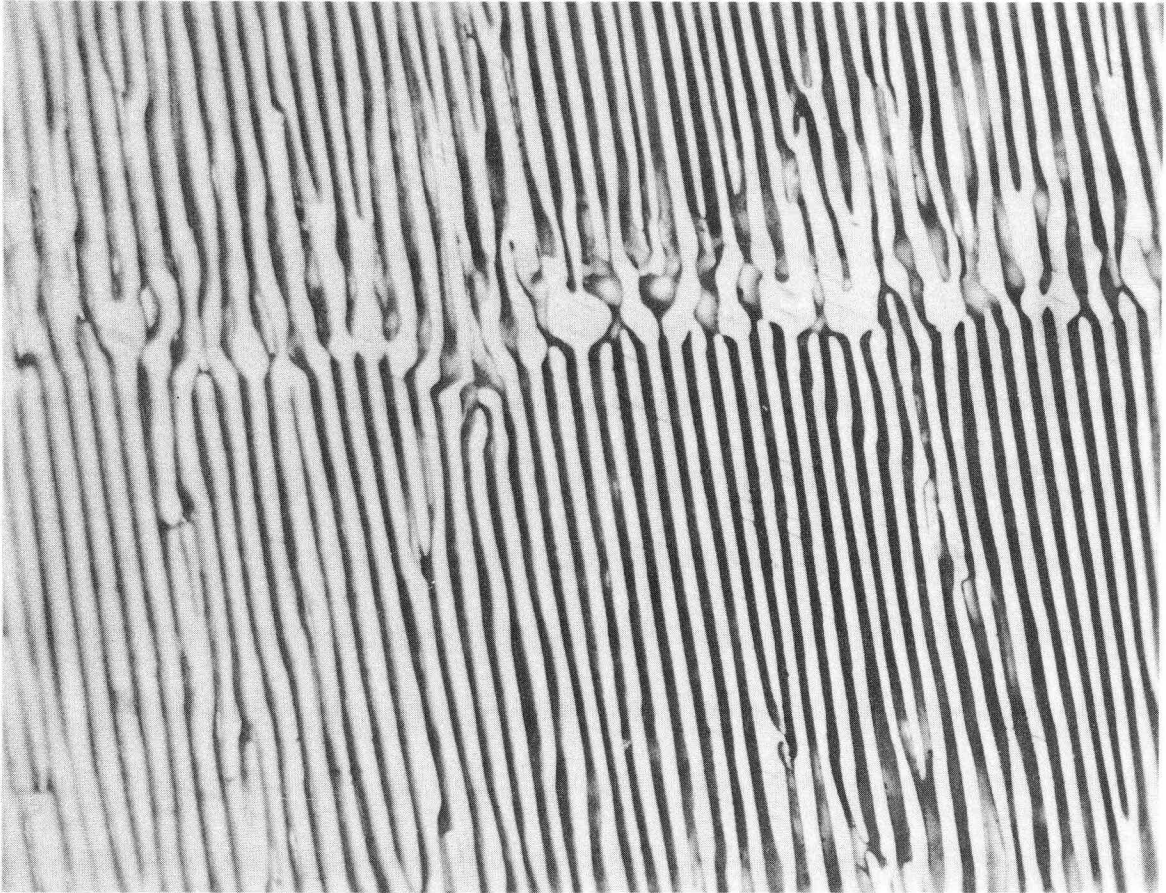
The regular lamellar structure of the Al-CuAl₂ eutectic was observed in most of the specimens near the end where solidification occurred last. This structure is shown in Fig. 3. Lamellar faults of the type shown at the right in the figure indicated that the solidification velocity was essentially constant in the region of the mold far from the water chill.

The band microstructure in those specimens exhibiting narrow bands is shown in Figs. 4 and 5, taken from different specimens. The microstructure of these bands is similar to that reported by earlier investigators,^{6,7,7a} in which the interlamellar spacing λ changes to a larger value over a short length. The interlamellar spacing following the band is smaller than that preceding the band, as shown in both of these figures, although the effect is more pronounced in Fig. 5. The band appears to be more rich in the light θ -CuAl₂ phase. The dark Al-phase lamellae tend to join in pairs at the initial side of the band before terminating. Some of the Al-phase lamellae extend through the band and nucleate additional lamellae of that phase in a manner similar to that shown in Fig. 3. Electron microprobe analysis was performed to measure the extent of the θ -phase enrichment. However, the enrichment was below the level of detection by this method (1%) indicating that the enrichment is only an optical effect.



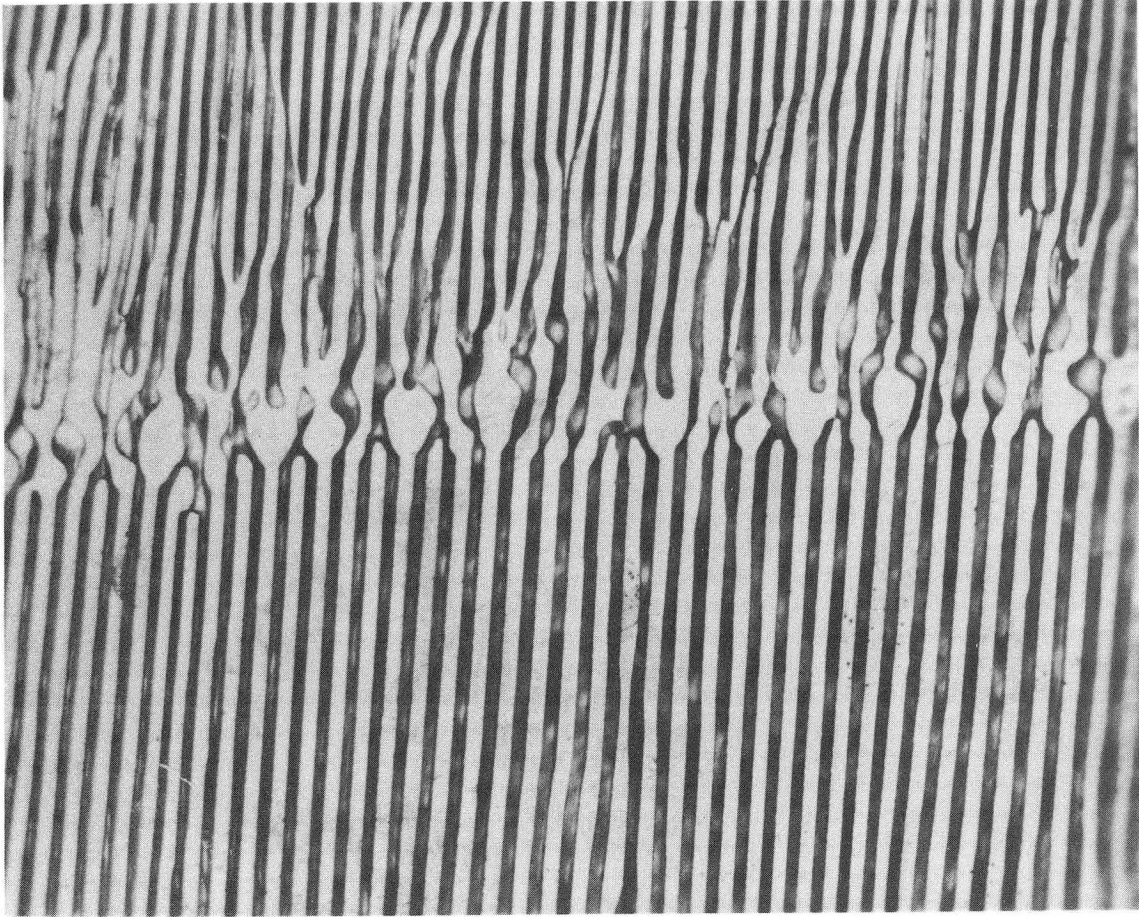
XBB 7210-5207

Fig. 3. Longitudinal micrograph showing lamellar structure without distortion. Growth direction from bottom to top.



XBB 7210-5210

Fig. 4. Longitudinal micrograph showing a band. Growth direction from bottom to top. Mag. 772x.



XBB 7210-5214

Fig. 5. Longitudinal micrograph showing a band. Growth direction is from bottom to top.
Mag. 772x

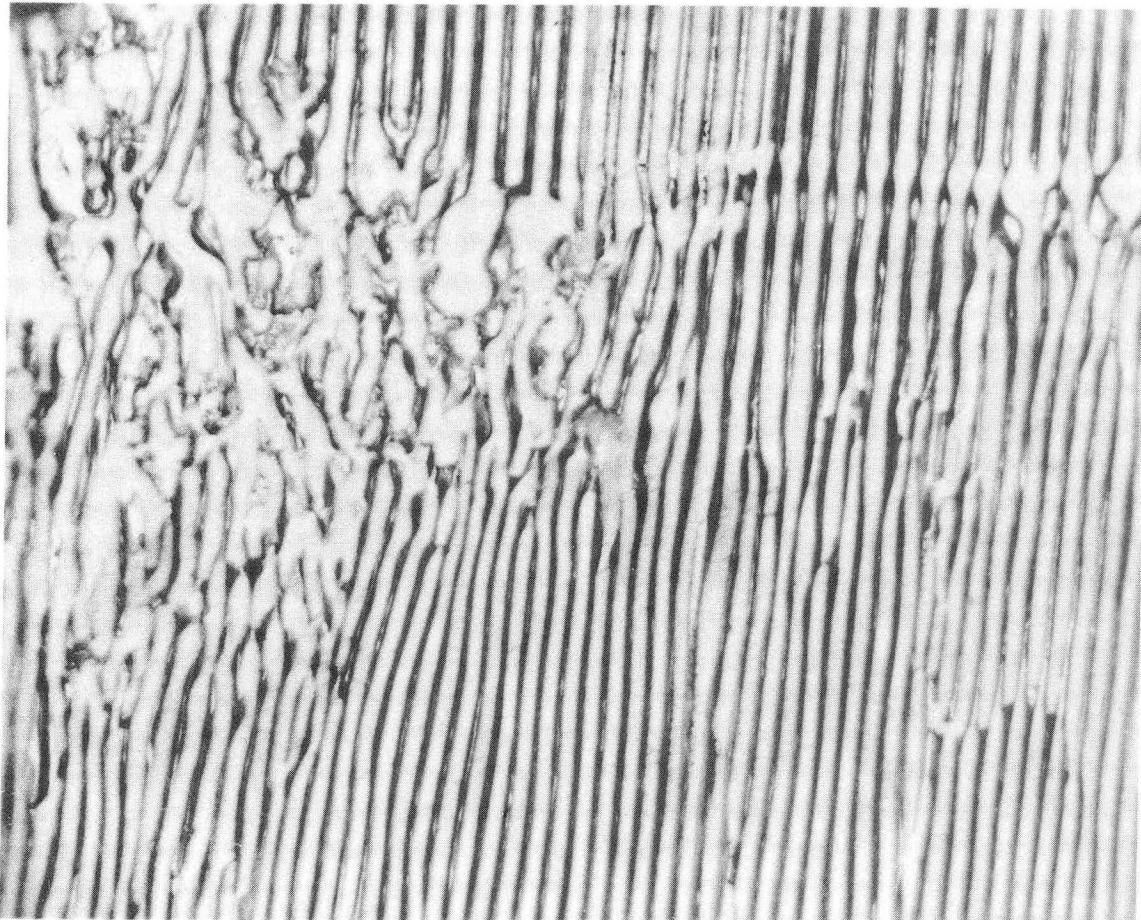
The band microstructure of the specimens showing varying band widths and broader bands is shown in Figs. 6 and 7, for different specimens. In the band shown in Fig. 6 part of the lamellar structure extends through the band, indicating that the thermal disturbance at the interface is localized. The slight variation in width of the Al-phase lamellae indicates the onset of a very small thermal fluctuation.

The band structure shown in Fig. 7 indicates that the thermal disturbance extended along the entire freezing interface. Again the band width increases in localized regions as shown by the disordered structure at the right of the figure center.

A transverse section through the specimen shown longitudinally in Fig. 6 is shown in Fig. 8. This figure shows two grain, one of which contains a high subgrain density. What appears to be a grain boundary separating the two grains consists of a series of lamellar faults in addition to a change in orientation. Note that immediately to the right of this boundary is a narrow region of the ordered lamellar structure. The interior of the grain on the right, however, is severely disordered.

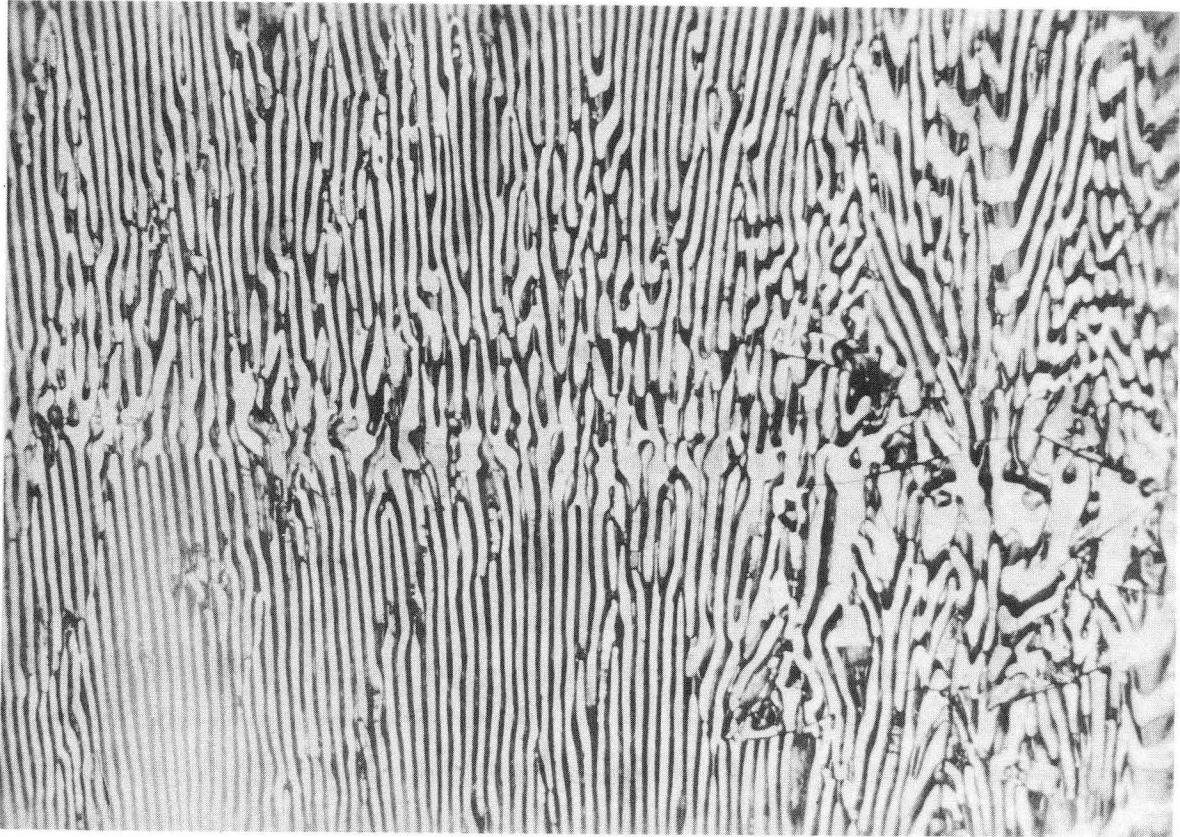
Figure 10 shows a higher magnification of the almost undisturbed part of Fig. 7. The small lines observed on Fig. 9 represent regions of mismatch⁶ (or subgrain boundaries). Figures 11 and 12 are transverse sections of specimens having narrow bands of the type shown in Figures 4 and 5.

These figures are presented to show more clearly the continuity of the phases across mismatched regions, or lamellar faults. The



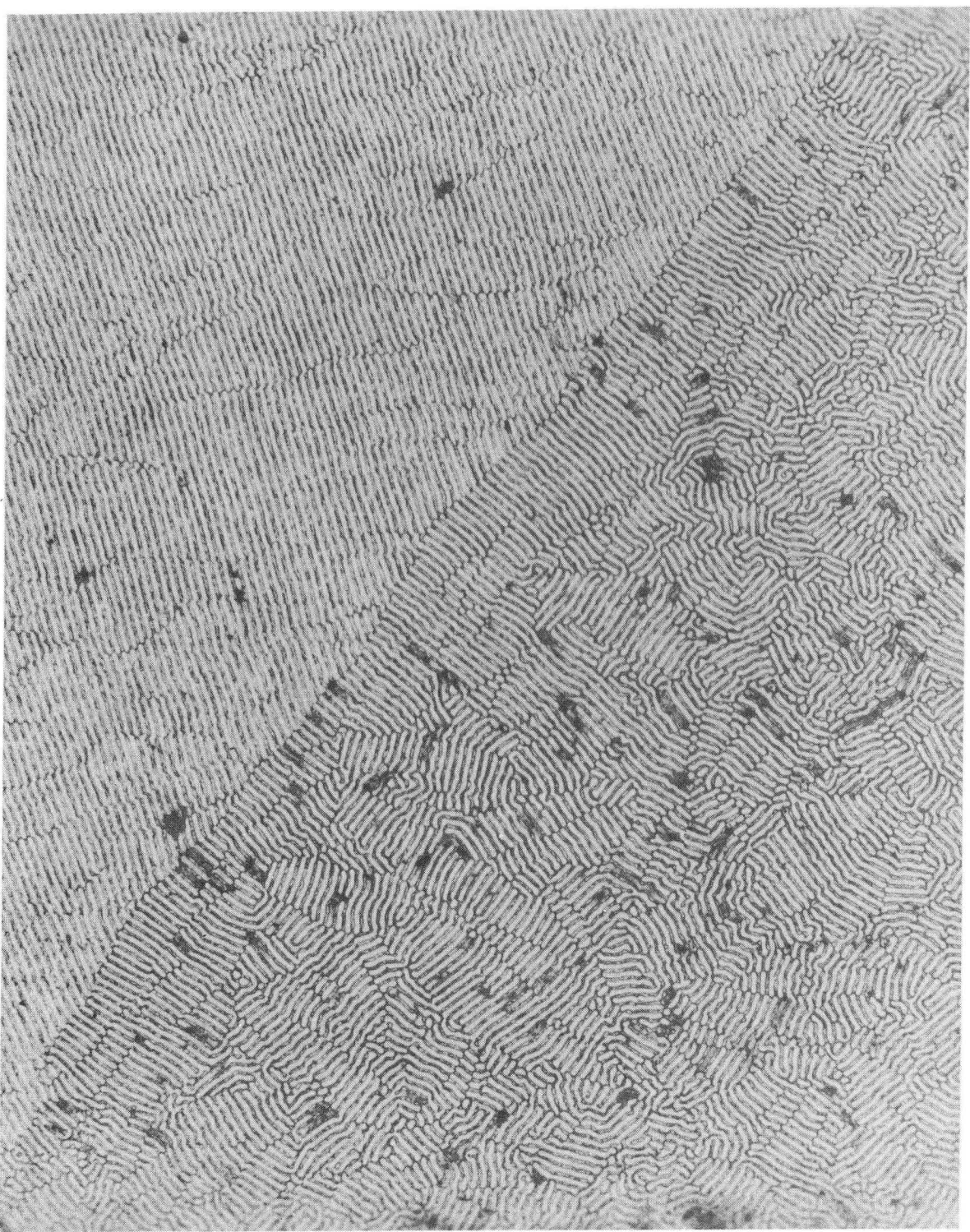
XBB 7210-5212

Fig. 6. Longitudinal section of unidirectionally solidified Al-CuAl₂ eutectic showing a banded structure. Growth direction is from bottom to top. Mag. 766x



XBB 7210-5208

Fig. 7. Longitudinal micrograph showing a band severely disturbed on one side. Growth direction from bottom to top.
Mag. 670x



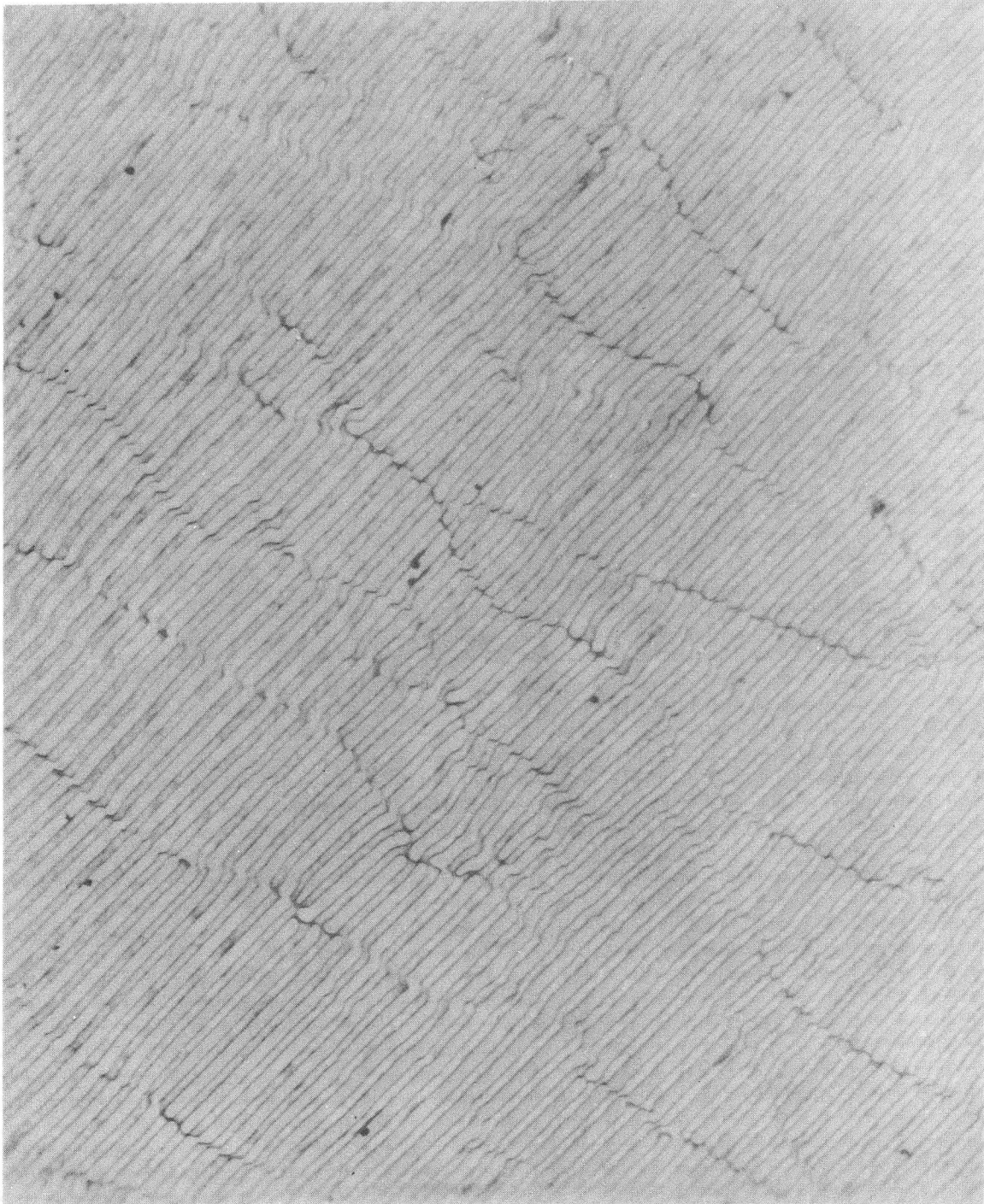
XBB 7210-5206

Fig. 8. Transverse micrograph of a band with one side severely disturbed in Al-CuAl₂ eutectic. Mag. 544x



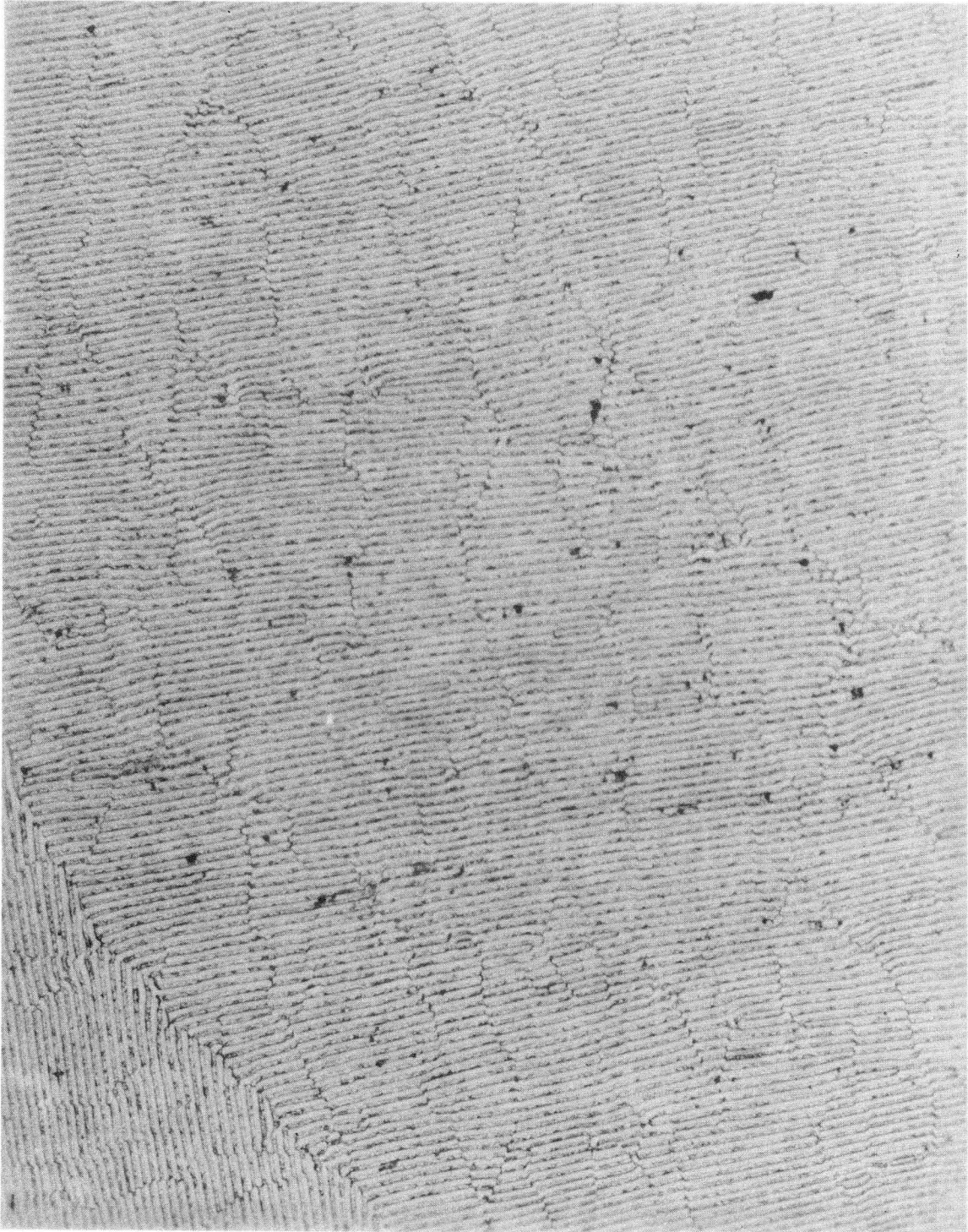
XBB 7210-5205

Fig. 9. Transverse micrograph showing a higher magnification of a sub-grain region which still maintains constant lamellar spacing. Mag. 1296x



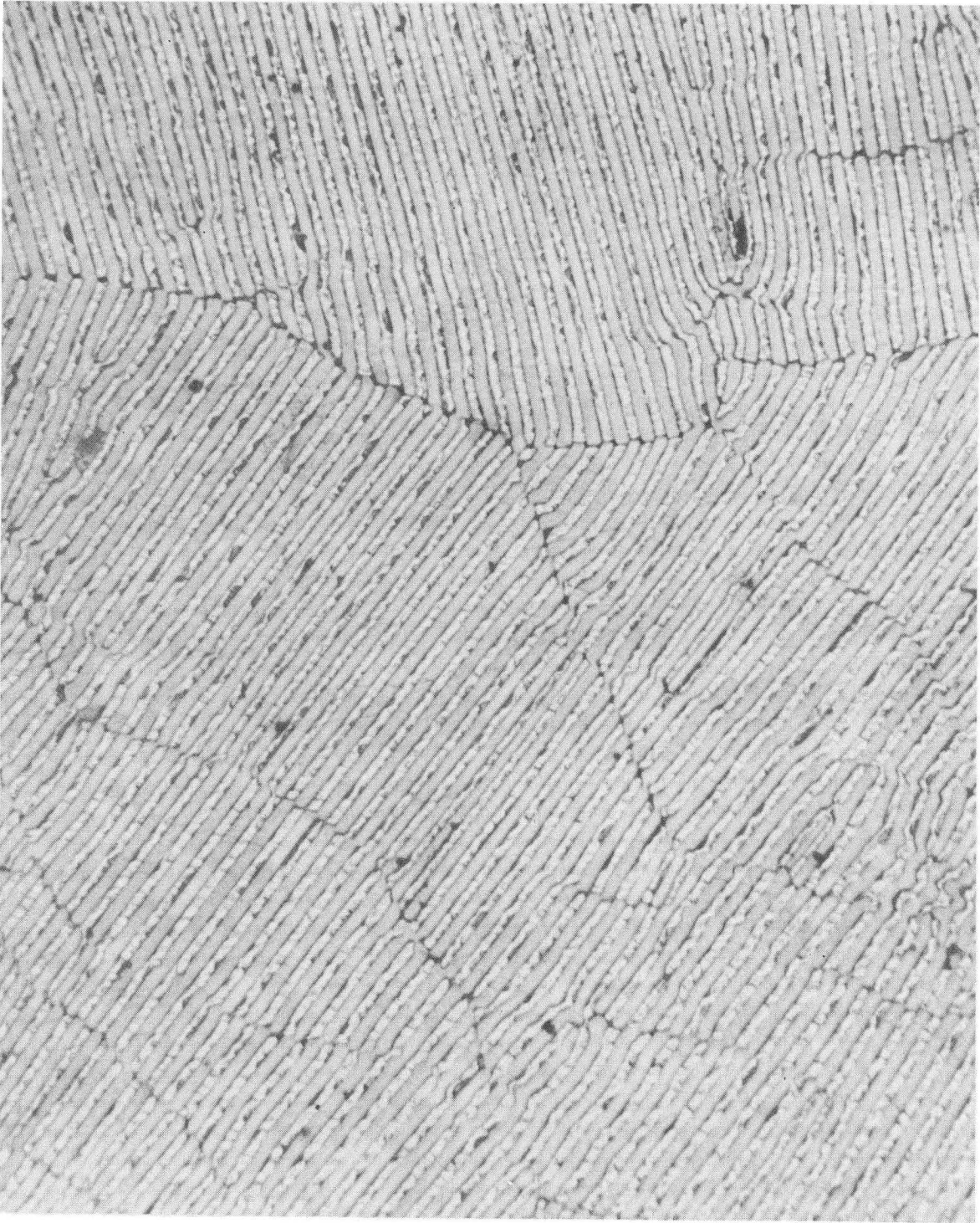
XBB 7210-5204

Fig. 10. Transverse micrograph of Al-CuAl₂ eutectic showing a higher magnification of the almost undisturbed part of Fig. 7.
Mag. 1220x



XBB 7210-5203

Fig. 11. Transverse micrograph of Al-CuAl₂ eutectic.
Mag. 542x

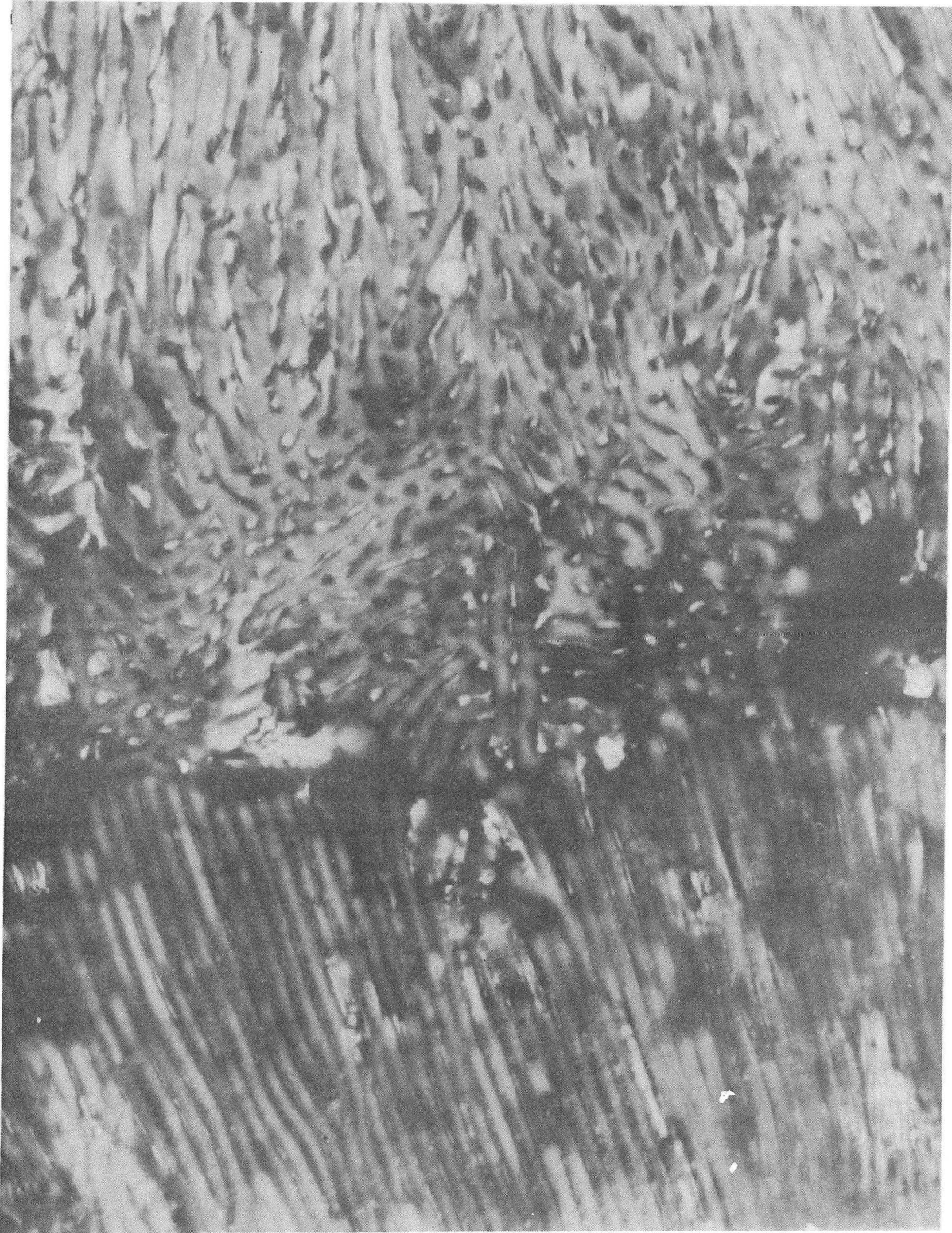


BB 7210-5209

Fig. 12. Transverse micrograph of Al-CuAl₂ eutectic.
Mag. 1188x

dendritic breakdown of the lamellar structure found in three of the specimens is shown in Fig. 13. The occurrence of this structure was unexpected as the alloys were all of the eutectic composition. The breakdown is followed by a sort of branched cellular structure.

In all the micrographs shown in Figs. 2-11, the dark spots are artifacts, tiny holes on the surface of the polished and etched specimens due to abrasive polishing in the brittle θ -phase. Thus, most of the spots appear in the light areas as expected.



XBC 726-3484

Fig. 13. Longitudinal micrograph showing a eutectic-dendritic breakdown at a band. Growth direction is from bottom to top. Mag. 1420x

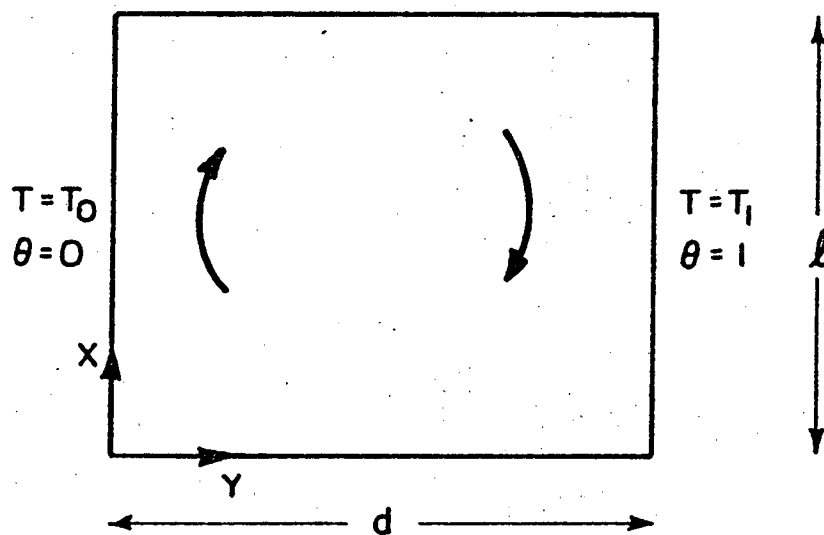
V. ANALYSIS AND DISCUSSION

It is believed that the banded microstructures presented in this paper were the result of convectional currents. These currents lead to periodic heat fluxes which vary with time across the liquid² and induce perturbations in the rate of advance of the solid-liquid interface for an otherwise steady-state growth. This has been observed to result in the formation of bands of different densities.² This agrees with the results of Chadwick⁷ who produced the banded structure by mechanically inducing the velocity perturbation. The variation with time of the perturbation and the hypothesis of Utech and Flemings²⁶ that concentration differences spaced less than 0.5 mm apart are eliminated by diffusion in the solid would account for some of the non-periodicity of the bands in Fig. 2.

A. Band Density Distributions

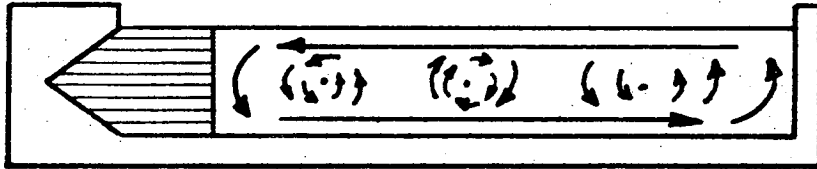
The fluid flow pattern in a liquid heated at the right and cooled on the left is shown in Fig. 15. This diagram corresponds to the fluid convection problem solved by Batchelor for a low thermal gradient. In the present a large thermal gradient was applied, giving rise to the periodic heat pulses and the existence of eddy currents shown schematically in Fig. 16. It is proposed that the banded region is produced by eddy currents which in turn cause growth velocity perturbations.

If eddy circulations in the melt are the source of the banding instabilities, then the banding density should decrease markedly as the length of liquid zone decreased with continued freezing. This



XBL 7212-7370

Fig. 15. Co-ordinate system and quantities involved in steady thermal convection between vertical surfaces of a two-dimensional rectangular enclosure.



XBL 7212-7371

Fig. 16. A schematic drawing of the eutectic solidification boat showing the actual pattern of fluid flow (eddy currents) within the melt during solidification.

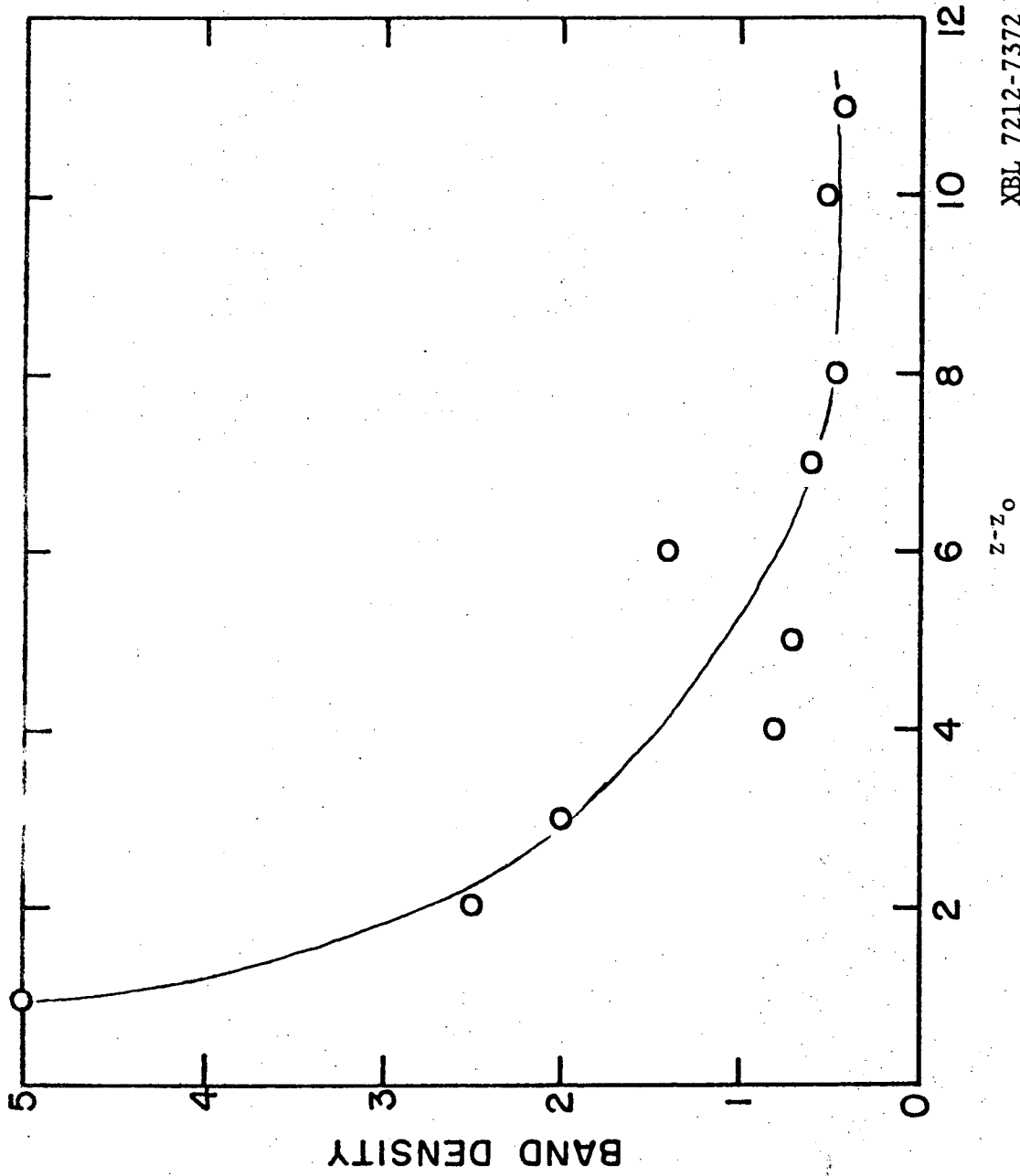
hypothesis was tested by measuring the relative density of bands as a function of distance along the solidification direction. These measurements are shown in Fig. 17. The density decrease shown in this figure and evident in Fig. 2, tend to confirm the turbulent convection origin of the observed bands.

It is significant to note that the nature of bands which were visible to the unaided eye appeared quite similar to the recent photographs of Vandebulcke and Vuillard² showing banded structures which resulted from convectional currents. Under the hypothesis of Kraft and Albright,⁶ the different types of bands could be explained by the presence of different types of impurities. Since a high purity eutectic alloy was used, no such impurities existed. Furthermore, no concentration pile-ups were detected by an electron microprobe analysis.

The difference in general microstructure of the specimens, some showing only narrow bands, some wide bands and others dendrites, could be explained on the basis of differences in nucleation at the chill end of the mold. Nucleation of multiple eutectic grains with unfavorable crystallographic orientations could induce subgrain boundary formation in some specimens. The variable grain size observed in different specimens suggests this contention.

B. Transient Interface Condition During Banding

The magnitude of thermal perturbations can be deduced from the dependence of the instantaneous interface temperature and freezing velocity dependence on the interlamellar spacing λ . Since λ is recorded continuously during solidification and can be measured directly from



XBL 7212-7372

Fig. 17. Density of band as function of distance along the directionally solidified ingot from the seed end. Solidification velocity is 216 cm/hr.

the micrographs, it is possible to deduce the transient state of the freezing interface through the band. For eutectic solidification it is known that the total interfacial undercooling is related to the freezing velocity V and interlamellar spacing λ by

$$\Delta T = K_1 V \lambda + K_2 \lambda^{-1} \quad (1)$$

Since ΔT tends toward an extremum in λ for a constrained freezing velocity, it can be shown that

$$\frac{\partial \Delta T}{\partial \lambda} = 0 \quad (2)$$

It follows that

$$\lambda^2 V = K_2 / K_1 = C_1 \quad (3)$$

and

$$\Delta T \lambda = 2K_2 = C_2$$

Here the constant K_1 is proportional to the liquid phase diffusivity D , while K_2 is the ratio of the Al-CuAl₂ interfacial energy $\gamma_{\alpha\beta}$ to the entropy of fusion for the eutectic, ΔS_f :

$$K_1 \propto D \quad (4a)$$

$$K_2 = \gamma_{\alpha\beta} / \Delta S_f$$

The constant C_1 has been measured by Chadwick⁷ from a graph of λ vs. $V^{-1/2}$ and found to be

$$C_1 = 7.4 \times 10^{-11} \text{ cm}^3/\text{sec} \quad (5)$$

Although the constant C_2 has not been determined for the Al-CuAl₂ eutectic, the magnitude can be estimated from the constant C_2 for the Sn-Pb eutectic. Hunt and Chilton^{37,38} found, that

$$C_2 = 7.5 \times 10^{-5} \text{ cm } ^\circ\text{C} \quad (6)$$

A better estimate of C_2 for the Al-CuAl₂ eutectic is obtained directly from the interfacial energy and entropy of fusion.

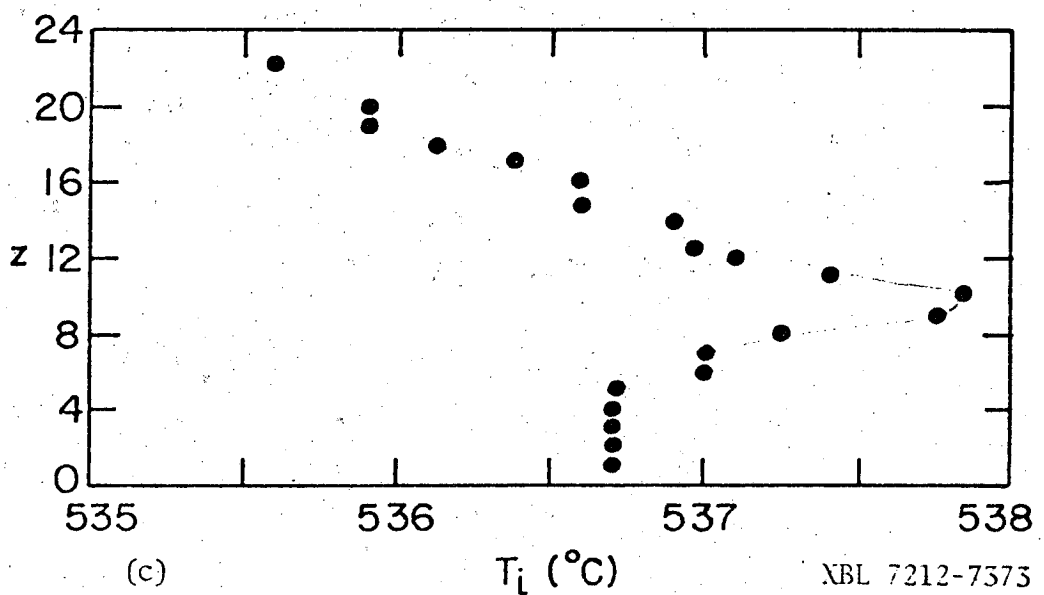
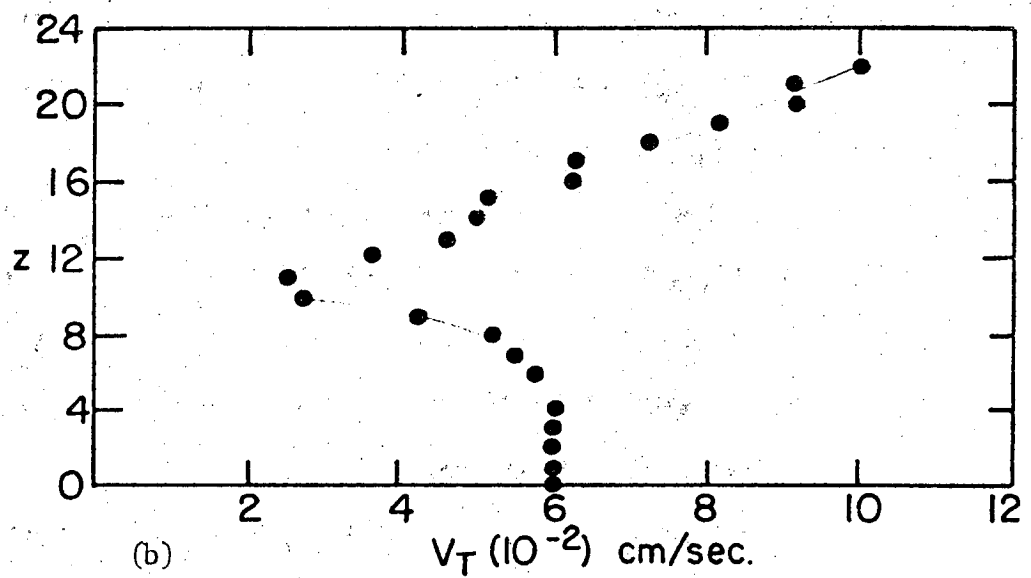
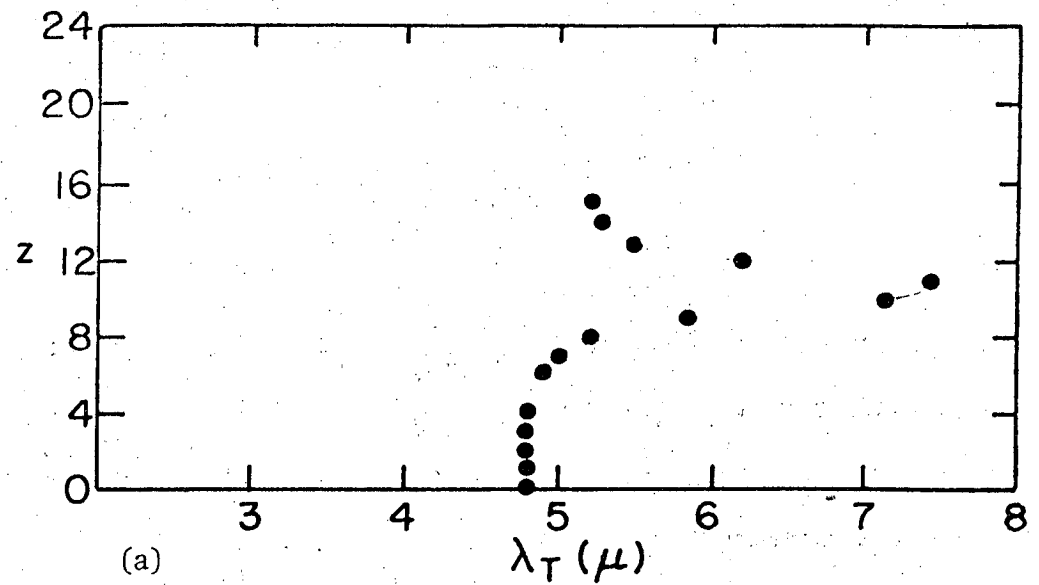
From the interlamellar spacing observed directly in the micrographs, it is now possible to deduce the instantaneous freezing velocity V and interface temperature T_i , given by

$$V = C_1/\lambda^2 \quad (7a)$$

$$T_i = T_m - C_2/\lambda \quad (7b)$$

where T_m is the melting temperature

The variation of the mean λ with position through the band shown in Fig. 5 is plotted in Fig. 18 along the transient growth velocity V_t and interface temperature T_i , as computed from Eqs. 7a and 7b. It is evident from the deduced form of T_i that a momentary increase in heat flux toward (or decrease in heat conduction away from) the interface occurred. Also from Eqs. 3, 7a, and 7b we see that as the interlamellar spacing λ , increases, both the velocity V , and the interface



NBL 7212-7575

Fig. 18. (a) Plot of λ_t vs. Z (in 3.2μ units)
 (b) Plot of V_t vs. Z (in 3.2μ units)
 (c) Plot of T_i vs. Z (in 3.2μ units)

undercooling ΔT , decrease whilst the interface temperature T_i increases indicating that the interface receives a momentary input of excess heat. The transient sources of the heat pulses are the eddy currents shown schematically in Fig. 16.

Note that because the average velocity is constrained by the constant motion of the furnace, a momentary decrease in the growth velocity must be followed by a transient increase above the average velocity V_{ave} . This post band transient is evident in Fig. 5, and shown by the calculated velocity function shown in Fig. 18b. Such changes in velocity will then account for the changes in λ spacing after a band. Thus where there is a transient increase above the average velocity V_{ave} one expects finer λ spacing as it is observed here. This is an obvious result of the Eq. 1, $\lambda^2 V = \text{const.}$

From the above discussion we see that as we move from one side of the band to the other, λ changes from an average constant λ_{ave} to a maximum on the band, then decreases to a value less than the λ_{ave} on the other side of the band. Then returns asymptotically to the value λ_{ave} . This can be seen from the fact that

$$\int_0^t v_t(t) dt = V_{ave} t$$

C. Subgrain Density Dependence on Band Spacing

The attainment of a constant λ value following the band depends on how closely the bands are spaced. When the band spacing is sufficiently closer together then the disorder in the lamellar structure does not anneal out before the next band occurs and also the reestablishing of the λ_{ave} value not be attained. The disorder tends to nucleate new disorder in the region beyond a band as shown in Fig. 7. If the band spacing is large however, then the disorder produced by the last band grows out of existence and the next band has a better chance to perpetuate the lamellar structure without significant disorder. Thus in a microstructure following a band it is probable for subgrain boundaries or mismatched regions to appear produced by renucleation of the lamellar structure, the subgrain boundary density decreases with continued growth as preferred orientation subgrains increase in size. The excess subgrain boundary energy drives the expansion of low energy grains or preferred orientation subgrains. In fact, Kraft et al.⁶ has shown that these mismatched regions are regions of high energy⁶ created by the fluid flow within the melt.

The idea that grains containing a high subgrain boundary density should exhibit a larger interlamellar spacing was tested for the microstructure shown in Fig. 8. The product $\Delta T \lambda = 2\gamma_{\alpha\beta} / \Delta S_f$ is a constant, and since the interface of both grains are at the same temperature ($\Delta T = \text{constant}$), then λ is directly proportional to $\gamma_{\alpha\beta}$. Measurements of the interlamellar spacing in Fig. 8 show that the transition region to the lower right of the grain boundary has surface energy $\sim 12.7\%$

smaller than that of the ordered grown at left whereas the center of the disordered region at the right has a surface energy $\sim 21.4\%$ larger.

D. Effect of Flow Separation on Variable Band Width

Lateral heat flow becomes increasingly important in altering the isothermal and streamline configurations for $\ell/d < 1$. In this experiment ℓ/d is of the order of 10^{-2} . Batchelor points out that in problems with low values of ℓ/d there is the possibility of breakdown of laminar flow near the ends of the cavity where the streamlines are curved. The circulation would therefore decrease with an increase of distance from the center of curvature. For these low values of ℓ/d the disturbance may have sufficient time to amplify and lead to flow separation. Thus, among the many processes occurring during irregular convection, the symmetry of flow in our rectangular mold is quite distorted and flow separation can lead to the observed structure in Fig. 6 which is representative of the specimens containing wide bands. The figure shows that flow was laminar before the separation since the structure was quite regular before the band. Immediately after the separation, one side remained laminar which leads to normal eutectic structure² whereas the other side entered a more turbulent phase lasting for about 0.25 second and the initially laminar region enters the turbulent phase for only ~ 0.02 second. This phenomenon in the specimen shown in Fig. 7. is similar except that the lamellar structure distortion was high. Figure 7 shows also that the disorder tends to increase following the band. The difference between the structures shown in Figs. 6 and 7 is that the lamellar spacing has decreased and become highly

distorted. This could be due to the fact that the previous disturbance had not annealed out or that the fluid motion had become more erratic or complex. The fact that one site on the band is more damaged than others indicates that the general fluid flow pattern remained the same as the one occurring for the structure shown in Fig. 7.

E. Dendritic Breakdown of the Eutectic

The microstructure of great interest is that shown in Fig. 13. As it was indicated such a structure has not been observed before in this eutectic. In addition to the work of Jordan and Hunt,⁸ Mollard and Flemings³⁶ had also found that a breakdown of a binary eutectic lead to a dendritic structure. The occurrence of this structure in three of the specimens is of great significance since the alloy used in all of this investigation was of the eutectic composition and not off eutectic. Jordan and Hunt, in studying Al-Cu alloys off the eutectic composition and growing with a eutectic structure, observed a eutectic-dendritic breakdown upon accelerating the growth rate. The significant observation here is the fact that this breakdown occurred at the eutectic composition and just on a band. It is believed that the breakdown observed in this study was the result of the various effects of the convectional currents within the melt.

VI. CONCLUSION

From the foregoing observations and discussion, it can be concluded that the rate of solidification of the crystal is not the only determining factor for banded structures and that banding can occur at very high growth rates $216 \text{ cm/hr} \gg 20 \text{ cm/hr}$ contrary to some earlier observations.

The existence of thermal convection has been used to explain all the microstructures observed. In fact, the structures could not be explained on any other known basis. The observation of Fig. 4 could not be explained by a mechanical velocity perturbation as was done by Chadwick since the band would not show the observed asymmetry under such conditions. This study has shown that band spacing depends on the length of the liquid zone. It has also been shown in this study that the degree of disorder depends on band spacing; the disorder decreases with large spacing. From the above observations and arguments, it is quite evident that the most likely conclusion to be drawn is that the banding structures were strongly linked to thermal convection instabilities and the various complex processes associated with them.

ACKNOWLEDGEMENTS

I would like to express my deep appreciation to Professors L. Donaghey and V. Zackay for their time, energy and support as members of the thesis committee during this work. The encouragements, pieces of advice and the many services too numerous to mention received from Professor R. H. Bragg, chairman of the thesis committee are deeply appreciated.

Special thanks go to the support staff of IMRD for all their help. The assistance of L. Johnson in the metallographic work and that of George Geogakopoulos in the electron microprobe analysis are gratefully acknowledged. I will also like thank Drs. A. S. Yue and W. Pfann for their helpful discussions.

The work was supported by the U. S. Atomic Energy Commission through the Inorganic Materials Research Division of the Lawrence Berkeley Laboratory.

REFERENCES

1. R. A. Laudise, The Growth of Single Crystal Solid State Phys. Series; Ed. Nick Holonyak Jr. 1970 Prentice Hall Inc., Englewood Cliffs, New Jersey.
2. L. Vandenbulcke and G. Vuillard, J. Crystal Growth 12 (1972) North-Holland Publishing Co. pp 137-144; 145-152.
3. H. P. Utech and M. C. Flemings, J. Appl. Phys. 37 (1966) p 2021
- 3b. Chalmers et al., Trans, TMS-AIME 1966, 236, p. 527.
4. J. R. Carruthers, J. Crystal Growth 2, (1968) p. 1-8, North-Holland Publishing Co., Amsterdam.
5. J. Szekely and P. S. Chhabra, Met. Trans. vol. 1, (May 1970) p. 1195.
6. R. W. Kraft and D. L. Albright, Trans. Met. Soc. AIME 221 (Feb. 1961) p. 95.
7. G. A. Chadwick, J. Inst. Metals 91 (1962-63) p. 169.
- 7a. A. S. Yue
8. R. M. Jordan and J. D. Hunt, J. Crystal Growth 11, (1971) 141-146 North Holland Publ. Co.
9. G. S. Cole, Trans. Met. Soc. AIME 239 (Sept. 1967) p. 1287.
10. K. S. Chang, R. G. Akins, L. Burris, Jr., S. G. Bankoff, Argonne National Laboratory, Report # ANL-6835.
11. A. Emery and N. C. Chu, Trans. ASME, (1965) 87, p. 110.
12. R. J. Goldstein and E. R. Eckert, Intern J. Heat Mass Transfer, (1960) 1, p. 208.
13. H. P. Oosthuizen, Appl. Sci. Res., (1966) 16, p. 121.

14. A. Szewczyk, Intern. J. Heat Mass Transfer, (1962) 5 p. 903.
15. T. Fujii, Bull. JSME, (1959) 2, p. 365.
16. T. Fujii, Bull. JSME (1959) 2 p. 559.
17. R. K. Soberman, Phys. Fluids, (1959) 2, p. 131.
18. J. P. Hartnett, W. E. Welsh, and F. W. Larsen, Preprint 27,
Session XX, Nuclear Engineering and Science Conference, Chicago,
1958.
19. J. P. Fraser and D. J. Oakley, Trans. ASME, (1957) 79, p. 1185.
20. E. R. G. Eckert and W. O. Carlson, Intern. J. Heat Mass Transfer,
(1961) 2, p. 106.
21. G. K. Batchelor, Quart. Appl. Maths. (1954) 12, p. 209.
22. U. H. Kurzweg, Intern. J. Heat Mass Transfer, (1965) 8, p. 35.
23. G. S. Cole and W. C. Winegard, J. Inst. Metals (1964-65) 93, p. 153.
24. J. R. Carruthers and W. C. Winegard, Crystal Growth, H. S. Peiser,
Ed., p. 645, Pergamon Press, (1967).
25. W. R. Wilcox and C. R. Wilke, Ultra Purification of Semi-Conductor
Materials, M. S. Brooks and J. K. Kennedy Eds., p. 481, MacMillan,
New York (1962).
26. H. Utech and M. C. Flemings, Crystal Growth, H. S. Peiser Eds.,
p. 651, Pergamon Press (1967).
27. A. Müller and M. Wilhelm, Z. Naturforsch (1964) A19, p. 254.
28. D. T. J. Hurle, Phil. Mag., (1966) 13, p. 305.
29. G. S. Cole and W. C. Winegard, Can. Met. Quart., (1962) 1, p. 29.
30. F. W. Weinberg, Crystal Growth, H. S. Peiser, Ed., p. 651
Pergamon Press (1967).

31. H. P. Utech, W. S. Browser, and J. G. Early, ibid., p. 201.
32. G. S. Cole, Ph. D. thesis, Univ. of Toronto, 1963.
33. H. P. Utech, D. Sc. thesis, Mass. Inst. Tech., (1965).
34. W. R. Wilcox and L. P. Fullmer, Report No. ATN-64(9236)-19, (1964)
Aerospace Corp., El Segundo, Calif.
35. W. R. Wilcox, Chem. Eng. Sci., (1961) 13, p. 113.
36. F. R. Mollard and M. C. Flemings, Trans TMS-AIME (1967) 239,
p. 1535.
37. Lee Donaghey, Ph.D. thesis, Stanford University, Palo Alto, Calif.
38. Hunt et al, J. Inst. Metals 91, (1962).

LEGAL NOTICE

This report was prepared as an account of work sponsored by the United States Government. Neither the United States nor the United States Atomic Energy Commission, nor any of their employees, nor any of their contractors, subcontractors, or their employees, makes any warranty, express or implied, or assumes any legal liability or responsibility for the accuracy, completeness or usefulness of any information, apparatus, product or process disclosed, or represents that its use would not infringe privately owned rights.

TECHNICAL INFORMATION DIVISION
LAWRENCE BERKELEY LABORATORY
UNIVERSITY OF CALIFORNIA
BERKELEY, CALIFORNIA 94720